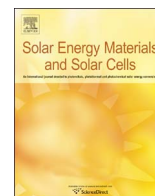




Contents lists available at ScienceDirect

## Solar Energy Materials &amp; Solar Cells

journal homepage: [www.elsevier.com/locate/solmat](http://www.elsevier.com/locate/solmat)

# CIGS solar cells on ultra-thin glass substrates: Determination of mechanical properties by nanoindentation and application to bending-induced strain calculation

Arnaud Gerthoffer<sup>a,\*</sup>, Christophe Poulain<sup>b</sup>, Frédéric Roux<sup>a</sup>, Fabrice Emieux<sup>a</sup>, Louis Grenet<sup>a</sup>, Simon Perraud<sup>a</sup>

<sup>a</sup> CEA, LITEN, 17 Rue des Martyrs, 38054 Grenoble Cedex 9, France

<sup>b</sup> CEA, LETI, MINATEC, 17 Rue des Martyrs, 38054 Grenoble Cedex 9, France

## ARTICLE INFO

### Keywords:

Cu(In,Ga)Se<sub>2</sub>  
Flexible  
Strain  
Nanoindentation  
Young's modulus  
Hardness

## ABSTRACT

Cu(In, Ga)Se<sub>2</sub> (CIGS) based thin film solar cells have been extensively studied and today, power conversion efficiencies higher than 20% have been demonstrated on both rigid and flexible substrates. However, very little is known about the mechanical resistance of flexible CIGS solar cells under flexion. Here we report an original study on the mechanical properties of CIGS solar cells fabricated on 100 μm-thick ultra-thin glass substrates. The Young's modulus and hardness of Mo and CIGS thin films are measured by nanoindentation, a technique well adapted to the characterization of thin film materials. Young's modulus values of 289 GPa and 70 GPa are obtained for the Mo and the CIGS layers respectively, as well as a CIGS hardness of 3.4 GPa. These values, combined with an analytical model, allow calculating the strain induced in thin film during the flexion of solar cells fabricated on ultra-thin glass substrate as well as on polyimide substrate. Thereby, we show that using a substrate with a low thickness and a low Young's modulus enables to lower the thin films strain during the flexion of cells.

## 1. Introduction

Flexible photovoltaic devices based on thin film technologies are highly desirable for the development of new applications as well as for a reduction of manufacturing costs through roll-to-roll processing. Among thin film solar cell technologies, the technology based on the Cu(In,Ga)Se<sub>2</sub> (CIGS) absorber material is one of the most promising since it has reached well established efficiencies higher than 20% in many groups [1]. Studies on the material electronic properties and deposition process have enabled a continuous improvement of the performance of solar cells fabricated with flexible substrates made of polyimide [2], metal [3,4], ceramic [5] and, more recently, on ultra-thin glass (UTG) [6]. In addition to their ability to convert light into electrical power, flexible solar cells have to withstand mechanical stresses, ideally without any performance degradation. Recent studies have been reported on the bending induced degradation of flexible solar cells based on amorphous silicon [7], perovskite [8,9] and lead sulfide [10] thin films. These studies point out a degradation behavior related to the bending radius and/or to the number of bending cycles. For the CIGS technology, the behavior of solar cells under repeated

flexions was observed by Chirilă *et al.* for solar cells made on 25 μm-thick polyimide substrates [11] and in our lab for solar cells made on 100 μm-thick UTG substrates [6]. On polyimide substrates, a relative efficiency decrease of only 4% is reported after 1,000 bending cycles applied with a radius of curvature of 20 mm, while on UTG substrates, a relative efficiency decrease of 20% is reported after 3 bending cycles applied with a radius of curvature of about 50 mm. These results indicate that the substrate properties could have a huge influence on the degradation of cells under flexion.

The mechanical behavior of flexible devices is related to the thickness and the Young's modulus of the thin films and the substrate. Knowing these parameters, it becomes possible to predict the strain induced in the materials as a function of the radius of curvature [12,13]. In this framework, it is desirable to assess the Young's modulus of the materials involved in the fabrication of CIGS solar cells, which have classically the following stacked structure: ZnO:Al/ZnO/CdS/CIGS/Mo/Substrate. The CdS layer has a negligible influence on the strain distribution in the bent structure because of its low thickness, so it will not be considered in the following. Young's modulus values between 290 and 330 GPa were reported for bulk Mo

\* Corresponding author.

E-mail address: [arnaud.gerthoffer@cea.fr](mailto:arnaud.gerthoffer@cea.fr) (A. Gerthoffer).

<http://dx.doi.org/10.1016/j.solmat.2016.11.022>

Received 31 August 2016; Received in revised form 14 November 2016; Accepted 18 November 2016

Available online xxxx

0927-0248/ © 2016 Elsevier B.V. All rights reserved.

[14,15] and Mo thin films sputtered on Si substrate [16], but lower values (133–172 GPa) were reported for Mo thin films sputtered on polyimide substrate [17]. In the same work, a CIGS Young's modulus of 73.4–83.6 GPa was measured by nanoindentation, but no details were given on the experimental procedure. More recently, a CIGS Young's modulus of  $70.4 \pm 6.5$  GPa was estimated from stress-strain measurements on CIGS nanopillar [18]. The Young's modulus of ZnO, measured by nanoindentation on thin films sputtered with different conditions, lies between 61 and 125 GPa [19] and a value of 110 GPa was reported for sputtered ZnO:Al thin films [20].

In order to complete these data and because mechanical properties of thin films could vary with the deposition conditions, here we report on the measurement of the Young's modulus ( $E$ ) of sputtered Mo and coevaporated CIGS thin films by nanoindentation, a technique well adapted to the determination of mechanical properties of thin films, for which conventional stress-strain measurements cannot be applied. This technique also allows the determination of the hardness ( $H$ ) of the materials, *i.e.* their ability to resist to plastic deformation. A Mo hardness of 6.5 GPa was measured by nanoindentation [15] and the CIGS hardness has never been reported yet. Then we use the previously measured Young's moduli to calculate the position of the neutral axis in solar cells and the strain induced in the thin films depending on the radius of curvature. The influence of the substrate properties is pointed out by calculating the strain with two different substrates: a 100  $\mu\text{m}$ -thick ultra-thin glass substrate and a 25  $\mu\text{m}$ -thick polyimide substrate.

## 2. Material and methods

### 2.1. Samples preparation

CIGS solar cells are often fabricated on sodalime glass (SLG) substrates because of its coefficient of thermal expansion (CTE) of  $8.9 \times 10^{-6} \text{ K}^{-1}$ , a value close to the CTE of CIGS (ranging between  $5.0 \times 10^{-6}$  and  $9.5 \times 10^{-6} \text{ K}^{-1}$  [21]) and because it contains Na, well-known to improve the cell efficiency by diffusing into the CIGS during its growth, at a substrate temperature close to 550  $^\circ\text{C}$  [22]. The samples were fabricated on 1.1 mm-thick SLG substrates (Goodfellow) and on 100  $\mu\text{m}$ -thick borosilicate UTG substrates (D263T, Schott). UTG is used in our lab as a substrate for the fabrication of lightweight and conformable CIGS cells. With a CTE of  $7.2 \times 10^{-6} \text{ K}^{-1}$ , the D263T glass has a lower CTE than SLG but is still suitable for CIGS cells [6]. The two kinds of substrate were cleaned in an ultrasonic bath with a detergent solution and rinsed with deionized water. The mechanical properties of Mo were measured on a Mo thin film deposited with a Perkin Elmer 2400 DC magnetron sputtering equipment on a SLG substrate (Mo/SLG sample). Although not measured, the properties of Mo deposited on UTG are expected to be the same as Mo deposited on SLG because the two substrates have a similar and low surface roughness (root mean square roughness  $< 1$  nm). Moreover, the samples are not intentionally annealed during the Mo deposition (temperature remained lower than 100  $^\circ\text{C}$ ), making negligible the thermal expansion difference between the substrates and limiting possible diffusion phenomena from the substrate. On the other hand, the nature of the glass can have a significant influence on the CIGS properties, as mentioned in our previous work [6]. Therefore we measured the Young's modulus and the hardness of two CIGS layers: a layer deposited on a Mo coated SLG substrate (CIGS/Mo/SLG sample) and another deposited on a Mo coated UTG substrate (CIGS/Mo/UTG sample), with Mo layers deposited in the same conditions. The CIGS thin films are deposited in an Alliance Concept EVA450 equipment with our standard 3-stage coevaporation process, described elsewhere [6].

### 2.2. Characterization techniques

The thickness of the Mo and the CIGS films were determined with a

Veeco Detktak 8 profilometer. The surface roughness and morphology as well as the height profile of the indented surfaces were characterized by atomic force microscopy (AFM) in tapping mode with a Bruker Innova equipment and by scanning electron microscopy (SEM) with a LEO 1530 equipment.

A MTS Systems Corp. nanoindenter equipped with a XP head system and a three-sided Berkovich diamond tip was used to perform the indentation tests. The indentation procedure consists in pressing the tip on the surface with an increasing load ( $P$ ) until the tip-apex reaches the desired penetration depth ( $h$ ). During the loading phase, the indented material undergoes elastic and plastic deformations. Then the tip is lifted off from the surface, leaving a residual mark due to the permanent plastic deformation of the material. The Young's modulus and the hardness of the indented materials are deduced from the load-penetration ( $P(h)$ ) curves and from the harmonic contact stiffness ( $S$ ), obtained with the dynamic Continuous Stiffness Measurement (CSM) method [23]. Before and after the measurements on the Mo and the CIGS samples, indentation tests were made on a reference fused silica sample, for which  $E$  and  $H$  are known, in order to make sure that the equipment is well calibrated.

### 2.3. Nanoindentation: theoretical models

For each penetration depth of the tip,  $E$  and  $H$  are related to the projected area ( $A_C$ ) of the contact between the tip and the sample, and to the harmonic contact stiffness ( $S$ ) through the following expressions:

$$H = \frac{P}{A_C} \quad (1)$$

$$\frac{1 - \nu^2}{E} = \frac{1}{E_C^*} - \frac{1 - \nu_i^2}{E_i} \quad (2)$$

$$E_C^* = \frac{S}{2} \sqrt{\frac{\pi}{A_C}} \quad (3)$$

where  $E_C^*$  is the apparent Young's modulus of the contact,  $E_i$  and  $\nu_i$  are respectively the Young's modulus and the Poisson's ratio of the tip ( $E_i = 1040 \text{ GPa}$  and  $\nu_i = 0.07$  for a diamond tip), and  $\nu$  is the Poisson's ratio of the measured material. The Poisson's ratio  $\nu$  of the Mo was fixed to 0.3, a value based on data reported in the literature 0.292–0.301 [16]. The Poisson's ratio of CIGS is not known, so it was also fixed to 0.3. As most of materials have a Poisson's ratio ranging between 0.0 and 0.4, the relative uncertainty induced on the determination of  $E$  from Eq. (2) is estimated to be less than 10%. For a perfect pyramidal indenter,  $A_C$  is related to the contact depth ( $h_C$ ) through the relation:

$$A_C = \pi h_C^2 \tan^2 \theta \quad (4)$$

where  $\theta$  is the half apical-angle of a conical indenter that would give the same projected contact area at a given  $h_C$ . For a Berkovich indenter,  $\theta = 70.32^\circ$ .  $h_C$  is the effective material height in contact with the tip. As sink-in or pile-up can occur during indentation,  $h_C$  depends on the behavior of the material and therefore should not be confused with the penetration depth  $h$  (see Fig. 1).  $h_C$  has a critical impact on the determination of mechanical properties and can be estimated with different classical methods [24–26]. However, an accurate estimation of  $h_C$  is sometimes challenging, in particular when indenting samples with rough surfaces. The surface roughness can also cause a wrong determination of the penetration depth, which is measured from the contact point between the tip and the surface. According to the ISO 14577 standard, the penetration depth has to be at least 20 times higher than the average surface roughness ( $R_a$ ) to make the relative uncertainty on the penetration depth lower than 5% [27]. When this criterion is not fulfilled, methods like the so called “ $dh_C/dh$  method” (see Section 2.3.2) are needed to avoid the influence of the surface roughness.

The two methods used in this contribution are described in the

Download English Version:

<https://daneshyari.com/en/article/4758857>

Download Persian Version:

<https://daneshyari.com/article/4758857>

[Daneshyari.com](https://daneshyari.com)